

LETTER • OPEN ACCESS

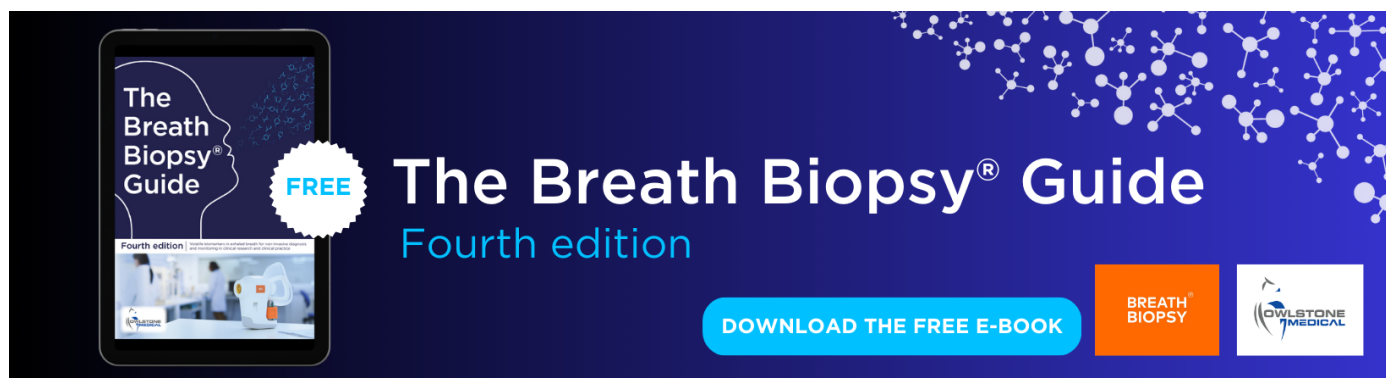
Urban NO_x emissions around the world declined faster than anticipated between 2005 and 2019

To cite this article: Daniel L Goldberg *et al* 2021 *Environ. Res. Lett.* **16** 115004

View the [article online](#) for updates and enhancements.

You may also like

- [Mortality-based damages per ton due to the on-road mobile sector in the Northeastern and Mid-Atlantic U.S. by region, vehicle class and precursor](#)
Calvin A Arter, Jonathan Buonocore, Charles Chang et al.
- [Evaluating current satellite capability to observe diurnal change in nitrogen oxides in preparation for geostationary satellite missions](#)
Elise Penn and Tracey Holloway
- [PM and NO_x emissions amelioration from the combustion of diesel/ethanol-methanol blends applying exhaust gas recirculation \(EGR\)](#)
Miqdam T. Chaichan, Noora S. Ekab, Mohammed A. Fayad et al.



The Breath Biopsy® Guide
Fourth edition

DOWNLOAD THE FREE E-BOOK

BREATH BIOPSY

OWLSTONE MEDICAL

ENVIRONMENTAL RESEARCH
LETTERS

LETTER

OPEN ACCESS

RECEIVED
24 June 2021REVISED
8 September 2021ACCEPTED FOR PUBLICATION
1 October 2021PUBLISHED
20 October 2021

Original content from
this work may be used
under the terms of the
[Creative Commons
Attribution 4.0 licence](#).

Any further distribution
of this work must
maintain attribution to
the author(s) and the title
of the work, journal
citation and DOI.

Urban NO_x emissions around the world declined faster than anticipated between 2005 and 2019Daniel L Goldberg^{1,*} , Susan C Anenberg¹ , Zifeng Lu² , David G Streets² , Lok N Lamsal^{3,4}, Erin E McDuffie⁵ and Steven J Smith⁶ ¹ Milken School of Public Health, George Washington University, Washington, DC, United States of America² Energy Systems Division, Argonne National Laboratory, Lemont, IL, United States of America³ Goddard Earth Sciences Technology and Research, Universities Space Research Association, Columbia, MD, United States of America⁴ NASA Goddard Space Flight Center, Greenbelt, MD, United States of America⁵ Department of Energy, Environmental, and Chemical Engineering, Washington University in St. Louis, St. Louis, MO, United States of America⁶ Joint Global Change Research Institute, Pacific Northwest National Laboratory, College Park, MD, United States of America

* Author to whom any correspondence should be addressed.

E-mail: dgoldberg@gwu.edu**Keywords:** urban, NO_x, OMI NO₂, emissions, satellite-basedSupplementary material for this article is available [online](#)

Abstract

Emission inventory development for air pollutants, by compiling records from individual emission sources, takes many years and involves extensive multi-national effort. A complementary method to estimate air pollution emissions is in the use of satellite remote sensing. In this study, NO₂ observations from the Ozone Monitoring Instrument are combined with re-analysis meteorology to estimate urban nitrogen oxide (NO_x) emissions for 80 global cities between 2005 and 2019. The global average downward trend in satellite-derived urban NO_x emissions was 3.1%–4.0% yr^{−1} between 2009 and 2018 while inventories show a 0%–2.2% yr^{−1} drop over the same timeframe. This difference is primarily driven by discrepancies between satellite-derived urban NO_x emissions and inventories in Africa, China, India, Latin America, and the Middle East. In North America, Europe, Korea, Japan, and Australasia, NO_x emissions dropped similarly as reported in the inventories. In Europe, Korea, and Japan only, the temporal trends match the inventories well, but the satellite estimate is consistently larger over time. While many of the discrepancies between satellite-based and inventory emissions estimates represent real differences, some of the discrepancies might be related to the assumptions made to compare the satellite-based estimates with inventory estimates, such as the spatial disaggregation of emissions inventories. Our work identifies that the three largest uncertainties in the satellite estimate are the tropospheric column measurements, wind speed and direction, and spatial definition of each city.

1. Introduction

Urban areas account for 55% of the global population and this number is expected to increase to 68% by 2050 (Ritchie and Roser 2018). In the future, city governments will have a larger fraction of air pollutant and greenhouse gas emissions under their purview, including nitrogen oxides (NO_x = NO + NO₂) and carbon dioxide (CO₂). Evaluating the history of air pollutant emission trends in urban areas gives insight on the effectiveness of past and current urban policies

to control these emissions, and gives a potential play-book for future policies.

Nitrogen dioxide (NO₂) is a deleterious air pollutant primarily resulting from the high-temperature combustion of fossil fuels (Jacob 1999). It is linked to increased incidence of pediatric asthma (Gauderman *et al* 2005, Khreis *et al* 2017, Achakulwisut *et al* 2019), and respiratory-related mortality (Samoli 2006, He *et al* 2020). NO₂, itself a noxious compound, also photochemically reacts in the atmosphere in the presence of volatile organic compounds to create ozone

(O₃) and fine particulate matter (PM_{2.5}), additional harmful pollutants (Jacob 2000).

NO₂ observations from satellite instruments have been informing the scientific community since the late 1990s (Burrows *et al* 1999, Leue *et al* 2001, Richter and Burrows 2002, Martin 2003). Utilizing observations from polar-orbiting satellite instruments can be especially powerful since a single instrument makes global measurements, as opposed to bottom up inventories that are built from a variety of reported datasets and vary in their rigor spatially. Satellite data are perhaps most often used in the quantification of long-term trends of NO₂ concentrations (Duncan *et al* 2016, Krotkov *et al* 2016, Georgoulas *et al* 2019). Because of the short NO₂ lifetime during the daytime (2–8 h), NO_x emissions are highly correlated with NO₂ column amounts (Stavrakou *et al* 2008, Kim *et al* 2009, Lamsal *et al* 2011, Duncan *et al* 2013). For this reason, satellite data have often been used to evaluate NO_x emissions inventories.

Decreases throughout North America and Europe and recent emission reductions in China have been reported in widely used bottom-up inventories. In North America and Europe, satellite-based studies have shown that regional NO_x emissions have dropped at a rate of approximately 3%–7% yr^{−1} since 2005 (Castellanos and Boersma 2012, Lu *et al* 2015, Zhang *et al* 2018, Silvern *et al* 2019, Goldberg *et al* 2019a, Macdonald *et al* 2021, Zara *et al* 2021) leading to 30%–70% reductions over a 15 year period. In China, there was a rapid NO_x emissions increase in the 2000s (Richter *et al* 2005), peaking in 2012, and a subsequent decrease thereafter (Reuter *et al* 2014, De Foy *et al* 2016, Li *et al* 2018, Zheng *et al* 2018, Wang *et al* 2019). Elsewhere NO_x emission trends have been mixed but generally have increased since 2005 (Lu and Streets 2012, Mahajan *et al* 2015, Duncan *et al* 2016, Geddes *et al* 2016, Barkley *et al* 2017, Georgoulas *et al* 2019, Itahashi *et al* 2019, Huneus *et al* 2020, Hickman *et al* 2021, Vohra *et al* 2021). Going forward, Elguindi *et al* (2020) summarize that past scenarios that assumed strong pollution controls best represent the documented trends in the United States, Europe, and China, while low pollution control scenarios lie closest to actual trends in developing regions such as India and West Africa.

Top-down statistical methods to infer urban NO_x emissions from satellite observations were originally developed using Ozone Monitoring Instrument (OMI) NO₂ data in the 2005–2009 timeframe (Beirle *et al* 2011). Beirle *et al* (2011) quantified NO_x emission rates from eight megacities. While satellite-based urban NO_x emissions showed general agreement with city-reported inventories, Riyadh had a factor of three larger emissions rate than the reported inventory. The method utilized by Beirle *et al* (2011) has subsequently been validated and refined on known NO_x emissions from power plants (De Foy *et al* 2015, Goldberg *et al* 2019b, Liu *et al* 2020). These studies

find that the Beirle *et al* (2011) method performs best on the largest sources (uncertainties <30% for sources >10 Gg yr^{−1} NO_x), which have a consistent daily signal that is larger than the values ~100 km upwind. Although the uncertainties can be fairly large for power plants, it is reasonable to think that the uncertainties for urban areas could actually be smaller because urban plumes are larger and more distinct from the upwind concentrations. An advantage of this technique over others (Canty *et al* 2015, Harkey *et al* 2015, Cooper *et al* 2017, Itahashi *et al* 2019, Visser *et al* 2019, Qu *et al* 2020) is that it does not rely on a chemical transport model, which are valuable tools, but involve an added layer of expertise and can be affected by model accuracy. Many prior studies quantifying NO_x emissions using this top-down method apply it on a subset of megacities or power plants (generally fewer than ten) (De Foy *et al* 2015, Lu *et al* 2015, Lorente *et al* 2019, Goldberg *et al* 2019b, Liu *et al* 2020) due to computational expense, but here we exploit recent computational capabilities to apply the Beirle *et al* (2011) method to a larger set of urban areas (189 cities) during a longer time-frame (15 years). We also provide an evaluation in these regions against NO_x emission estimates from multiple global bottom-up emission inventories.

2. Data and methods

2.1. OMI NO₂

OMI is a passive spectrometer launched on the NASA Aura satellite in July 2004 and has been providing global observations of NO₂ atmospheric column densities since 1 October 2004 (Levelt *et al* 2018). Aura is situated in a polar-orbiting flight path approximately 700 km above the Earth's surface with a Equatorial crossing time of 13:45 local time (Levelt *et al* 2006). Each day Aura has 14–15 orbits and was designed to have global coverage every day. Since the development of the 'row anomaly' in 2007 (Dobber *et al* 2008), which obstructs ~30% of the field of view, it now has global coverage once every 2–3 days. OMI NO₂ slant column densities are derived from backscattered radiance measurements in the 402–465 nm spectral window of the UV–Vis spectrometer (Marchenko *et al* 2015, Lamsal *et al* 2021). OMI measures backscatter radiances in a 2600 km swath with a nadir (center of the swath) pixel size of 13 × 24 km². The consistency of the data record over a 16+ year period has allowed for numerous long-term evaluations of trace gas species (McLinden *et al* 2016, Levelt *et al* 2018, Liu *et al* 2018, Abad *et al* 2019, Shen *et al* 2019, Silvern *et al* 2019, Goldberg *et al* 2019a).

OMI NO₂ data version 4.0 are operationally released by NASA (Lamsal *et al* 2021) (https://disc.gsfc.nasa.gov/datasets/OMNO2_003/summary). The version 4.0 update includes a high-resolution surface reflectivity product in the calculation of the air mass factor and a recently updated cloud scheme,

but still has a low bias of approximately 50% in urban areas when compared to column observations from *in situ* measurements. We filter the Level 2 OMI tropospheric column NO₂ data to ensure only valid pixels are used. Daily pixels with solar zenith angles $\geq 80^\circ$, cloud radiance fractions ≥ 0.5 , and surface albedo ≥ 0.3 are removed as well as the five largest pixels at the swath edges (i.e. pixel numbers 1–5 and 56–60). We also remove any pixel flagged by NASA including pixels with missing values and those affected by the row anomaly. The daily data are then re-gridded to a global $0.1^\circ \times 0.1^\circ$ grid.

The uncertainty in any daily measurement in the operational data has been assigned to be approximately 1.0×10^{15} molecules cm⁻² (Krotkov *et al* 2017). This equates to roughly a 5%–20% uncertainty over polluted areas. However, because we are over-sampling over many days (>100 days), we assume that random errors will cancel due to the large number of observations used (Russell *et al* 2010). This leaves only the systematic errors, such as the air mass factor bias in urban areas, which we discuss in section 2.4.

2.2. OMI NO_x emissions calculation

We use a top-down inverse statistical modeling technique to derive NO_x emissions from a combination of satellite data and re-analysis meteorology. In this method, all OMI NO₂ data over individual city centers or ‘hotspots’ are compiled and rotated based on the daily-observed wind direction, so that the over-sampled plume is decaying in a single direction. We utilize the 100 m wind speed and direction from the ERA5 re-analysis dataset (Hersbach *et al* 2020) generated at $0.25^\circ \times 0.25^\circ$. For each city we use the closest gridded value without interpolation.

This top-down method can only be applied when NO₂ is photochemically active and the NO₂ lifetime is short. Wintertime has more erroneous data due to snow cover and the longer NO₂ lifetime during wintertime yields urban plumes that are much more likely to overlap; both factors cause issues with the statistical fit. Therefore, we only use OMI NO₂ data from May to September in the Northern Hemisphere north of 25° N, November–March in the Southern Hemisphere south of 25° S, and all monthly data in Equatorial regions between 25° N and 25° S. We do not expect any significant systematic biases due to this temporal filtering. We aggregate all daily satellite data into 3 year averages; 36 months of data for tropical regions and 15 months of data for extratropical regions. We choose 3 year averages in lieu of 1 year or a shorter timeframe in order to average out the noise in daily measurements and to account for the row anomaly which causes fewer available measurements in the later time record.

Once all daily plumes have been rotated to be aligned as an effective horizontal plume and averaged together during a three year period (usually 100–600 snapshots), we integrate $\pm 0.5^\circ$ along the *y*-axis about

the *x*-axis to compute a one-dimensional line density in units of mass per distance. The line densities, which are parallel to the wind direction, peak near the primary NO_x emissions source and gradually decay downwind as the NO_x is transformed into different chemical species or deposited to the surface.

The line densities are fit to a statistical exponentially modified Gaussian (EMG) model (Beirle *et al* 2011, Valin *et al* 2013). This particular method was chosen due its ability to convert NO₂ column information into NO_x emission rates while accounting for meteorological influences and due to the multitude of studies verifying the methodology (De Foy *et al* 2014, Verstraeten *et al* 2018, Goldberg *et al* 2019c). A full description of the method can be found in the supplementary. An illustrative example of the method applied to Paris is shown in figure S1 (available online at stacks.iop.org/ERL/16/115004/mmedia). The five output parameters of the statistical fit are the: NO₂ burden, NO₂ background, decay distance, horizontal location of apparent source (ideally at the origin), and sigma of the Gaussian plume. The NO_x emissions rate from the source can be calculated from the NO₂ burden, decay distance, and NO_x/NO₂ ratio, which is assumed to be 1.33 (Beirle *et al* 2011, Valin *et al* 2011). In two final adjustments, the derived NO_x emissions are multiplied by a factor of 1.37 (Goldberg *et al* 2019c) due to a known low bias in urban areas caused by coarse resolution *a priori* vertical profile information incorporated in the air mass factor, and then by a factor 0.77 to account for an early afternoon high bias in the emissions rate compared to the 24 h average emissions rate reported by annual inventories, using diurnal allocation factors described in Denier Van Der Gon *et al* (2011); sensitivity analyses of the early afternoon adjustment factor can be found in the supplementary. A discussion of the uncertainties associated with all multiplicative factors are noted in section 2.4 and the supplementary.

2.3. Bottom-up emissions estimates

We acquired gridded anthropogenic total NO_x emissions data from five widely used inventories and projections (table 1): the Community Emissions Data System (CEDS) (McDuffie *et al* 2020), the Emissions Database for Global Atmospheric Research (EDGAR) version 5.0 (Crippa *et al* 2020), the Evaluating the Climate and Air Quality Impacts of Short-Lived Pollutants (ECLIPSE) version 5a (Klimont *et al* 2017), the Monitoring Atmospheric Composition and Climate CityZen (MACCity) project (Lamarque *et al* 2010), and the Shared Socioeconomic Pathways (SSP) projections (Riahi *et al* 2017). The two SSP scenarios displayed herein represent sustainability (SSP 1–1.9) and continued fossil fuel development (SSP 5–8.5) pathways.

The five inventories and their trends by region are shown in the supplementary (figures S2 and S3). In some cases, sectoral emissions needed to be added

Table 1. Summary of emissions inventories used for this study.

Inventory	First year	End year	Resolution	Increment	Projection?
CEDS ^a	1970	2017	$0.5^\circ \times 0.5^\circ$	Annual	No
EDGAR v5.0 ^b	1970	2015	$0.1^\circ \times 0.1^\circ$	Annual	No
MACCity ^c	1990	2020	$0.5^\circ \times 0.5^\circ$	Annual	Yes, projection from 2000
ECLIPSE v5a ^d	1990	2050	$0.5^\circ \times 0.5^\circ$	5 year	2020 only
SSP ^e	2005	2100	$0.5^\circ \times 0.5^\circ$	5 year	Yes, projection from 2005

^a <https://zenodo.org/record/3754964>

^b https://edgar.jrc.ec.europa.eu/gallery?release=v50_AP&substance=NOx§or=TOTALS

^c <https://eccad3.sedoo.fr/>

^d <https://iiasa.acat/web/home/research/researchPrograms/air/ECLIPSEv5a.html>

^e <https://esgf-node.llnl.gov/search/input4mips/>

together to create total anthropogenic NO_x emission files. The inventories report NO_x emissions as ‘equivalent’ NO₂, but the NO₂/NO_x ratio may vary by urban area, and can be considered a source of uncertainty. None of the inventories projected to 2020 include the effects of the COVID-19 lockdowns on air pollutant emissions.

All NO_x inventories are re-gridded to a common spatial resolution of $0.05^\circ \times 0.05^\circ$, while retaining all original values at the coarser spatial resolution. A final emissions output file is created which lists the NO_x emissions within radii of 0.1° to 0.75° at 0.05° increments of each city. We match the satellite-derived emissions to the emissions inventories using the sigma of the Gaussian plume which varies spatiotemporally. We assume that the satellite-derived emissions should be matched to a Gaussian radius of 2-sigma from the city center. The 2-sigma radius for all cities are provided in table S3. Varying the city radius between 1.5-sigma and 3-sigma will affect the magnitude comparison by $\pm 30\%$, but has a lesser effect on the trend comparison (figure S4).

2.4. Methodological uncertainties

The total error associated with the magnitude of the top-down vs. bottom-up comparison is calculated to be 53%, and is the sum of the quadrature of seven potential sources of error: the tropospheric vertical column measurement in urban areas (30%), the wind speed and direction (25%), the collocation of the spatial extent between the top-down fit and bottom-up emission inventory (30%), the early afternoon to 24 h conversion emissions rate (10%), the ‘clear-sky’ bias (10%) which for these purposes is a result of emissions being different on clear-sky days compared to cloudy days, the NO_x/NO₂ ratio (10%) (Kimbrough *et al* 2017), and the random error of the statistical EMG fit (10%) (De Foy *et al* 2014). This total uncertainty is comparable to Verstraeten *et al* (2018), who quantified an uncertainty of 55% using this method with OMI NO₂. For the trend analysis, the total uncertainty is much reduced, since the systematic uncertainties in the emissions

are consistent throughout the time period, thus leaving only the random EMG fitting error of roughly 10% (De Foy *et al* 2014). For further information on this method or the uncertainties associated with this method, please see the discussion in the supplementary or other literature (De Foy *et al* 2014, Lu *et al* 2015, Verstraeten *et al* 2018, Goldberg *et al* 2019c).

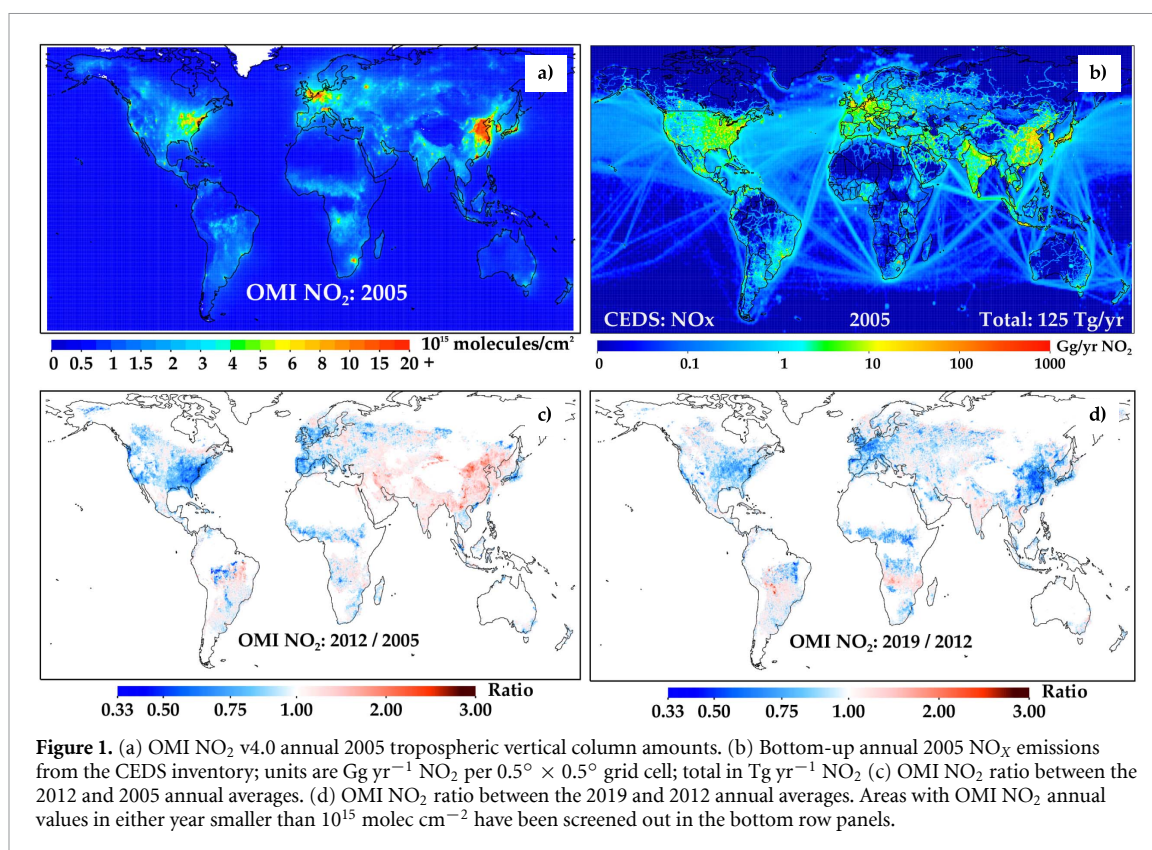
3. Results and discussion

3.1. OMI NO₂ trends

Regional NO₂ temporal trends since 2005 have been well-documented (Duncan *et al* 2016, Krotkov *et al* 2016, Georgoulias *et al* 2019). We update the findings here to include the most recent years of annual data, and to narrow the focus on urban NO_x emissions—instead of NO₂ concentrations. We purposefully exclude 2020 data due to the emission anomalies associated with the COVID-19 lockdowns. In 2005, the global regions with the largest anthropogenic emissions were: eastern United States, western Europe, and east Asia. This is documented by both the ‘top-down’ OMI NO₂ annual average of tropospheric vertical column NO₂ and the ‘bottom-up’ CEDS inventory (figure 1; note the non-linear colorbars in each panel).

Between 2005 and 2012, NO₂ concentrations dropped dramatically (25%–40%) in North America, western Europe, and Japan in response to stringent policies enacted to reduce NO_x emissions. Conversely, in China, India, and the Middle East, a lack of regional policies controlling NO_x emissions yielded a further increase (+10%–50%) in the NO₂ concentrations as compared to 2005 concentrations. Regional signals in Latin America, Africa, and Southeast Asia are mixed primarily due to the influence of biomass burning in these regions. In other locations, such as Central Asia, Northern Africa, and Oceania regional differences are dominated by natural variability due to sparse anthropogenic activities in these areas.

Between 2012 and 2019, NO₂ concentrations either dropped or held steady in most global regions. The largest decreases during this timeframe were



in eastern China. In very few regions, were there large obvious increases. NO₂ changes between 2005 and 2019 at the regional level are displayed in figure S5.

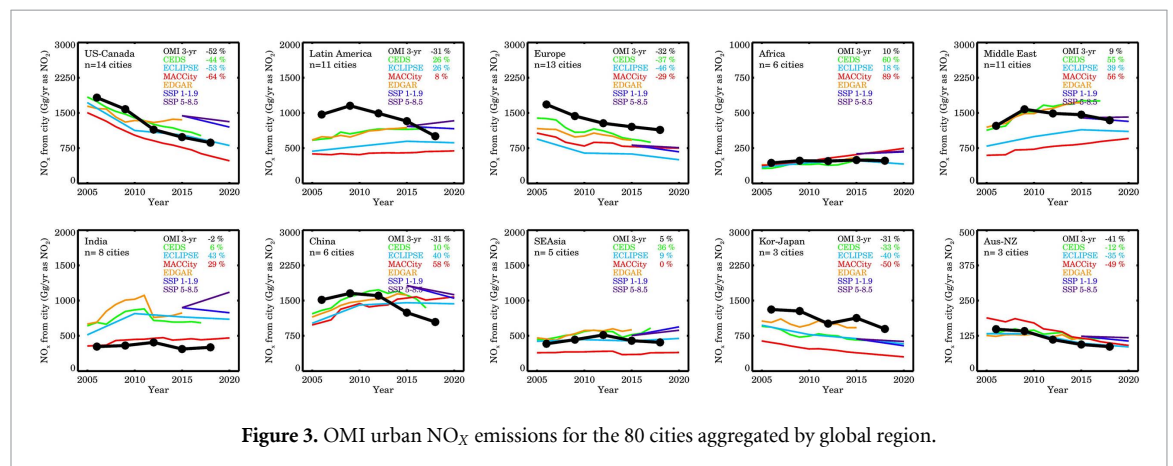
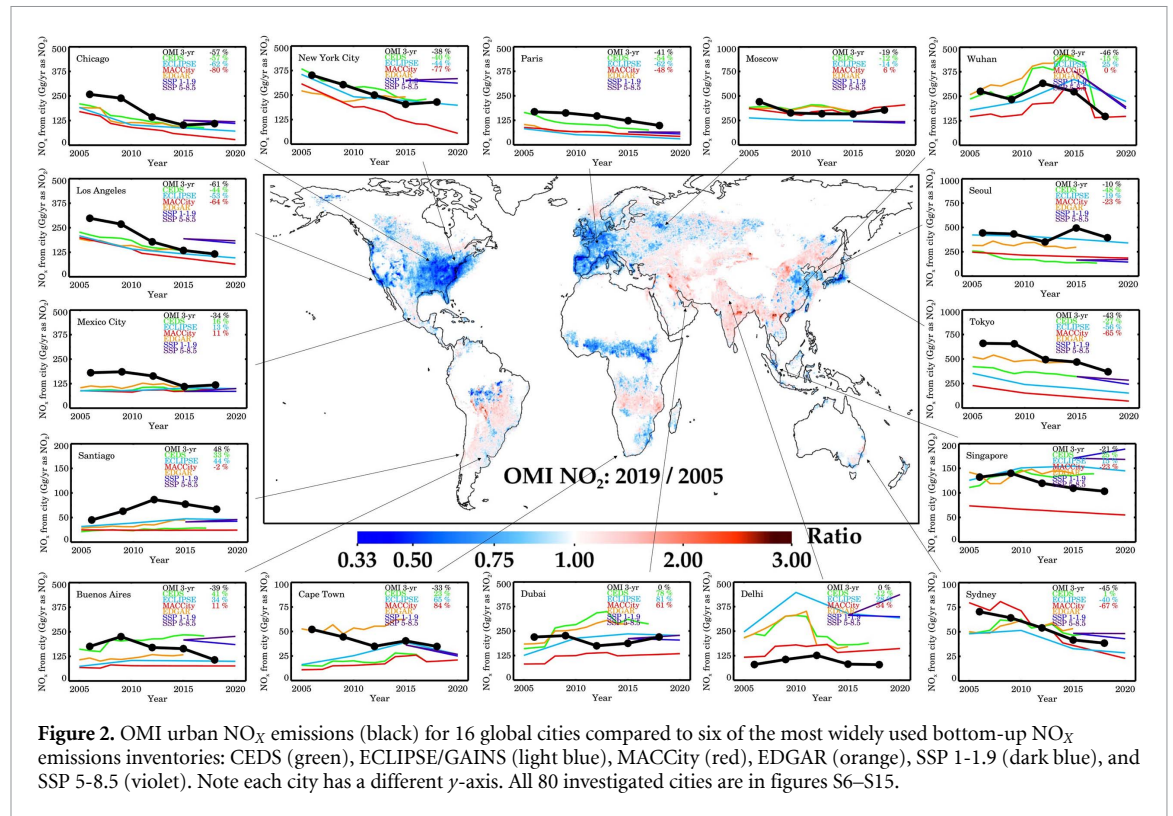
3.2. OMI NO_x emissions estimates for global megacities

Our top-down OMI NO_x calculation converged for 80 ($n = 80$) global cities for the 15 year period of interest (2005–2019); 16 of them are shown in figure 2. We first performed the analysis on the 97 C40 cities (www.c40.org/cities), and found that the method generally does not work for metropolitan areas with population sizes of <2 million residents because of OMI's lack of sensitivity to their daily NO₂ plumes. We then expanded our analysis to include all global urban areas with metropolitan area populations exceeding 2 million residents. In total, we performed the statistical fit on 189 global cities. In most cities (167 out of 189), the statistical fit converged in at least one out of the five 3 year periods of interest, but many cities did not have a full temporal range or the statistical fit would yield an unreasonably small effective NO₂ lifetime (<0.5 h) and unusually large sigma (>100 km); these instances were excluded from our analysis because discontinuous estimates are harder to screen for reliability and trend consistency. Our method only works for cities isolated from other large cities within a 200 km radius. Examples of cities in which this method does not work due to insufficient isolation are Beijing, Shanghai, Kinshasa,

Amsterdam, Boston, and Washington DC. The comparison between top-down OMI NO_x emissions and the five bottom-up emissions inventories for all 80 cities can be found in figures S6–S15. We anticipated that C40 cities, a group of cities pursuing high ambition climate action, would have larger NO_x reductions but we found no statistical difference between the trends in C40 cities and non-C40 cities since 2009 (figure S16).

When the 80 cities are grouped by region, patterns begin to emerge (figure 3). In the United States and Canada, top-down OMI NO_x estimates were available for 14 cities ($n = 14$), and when combined together, matched the bottom-up inventories in both trend and magnitude to within $\pm 10\%$; therefore, we assert no consistent bias in the urban NO_x inventories for these two countries. Similarly, excellent agreement was generally found in Australia and New Zealand.

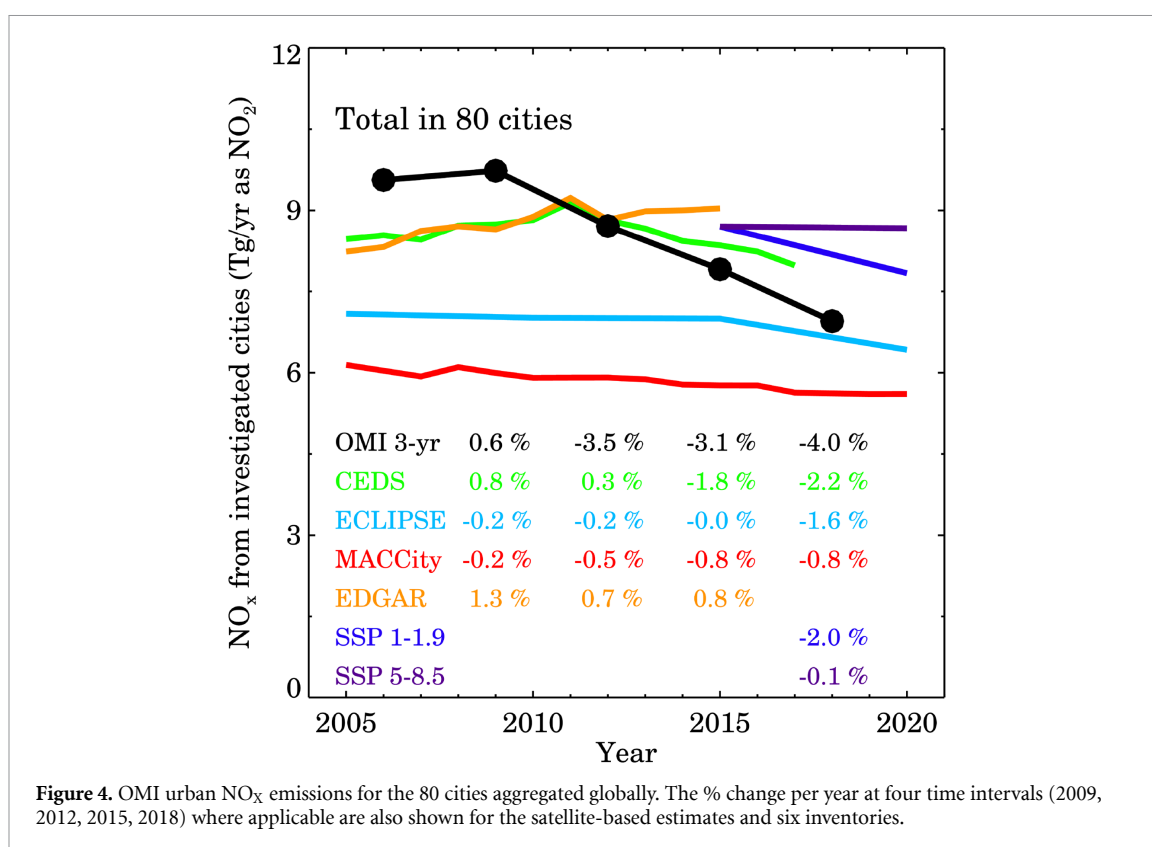
In Europe ($n = 13$) and South Korea/Japan ($n = 3$), the temporal downward trends of NO_x emissions match to within $\pm 10\%$, but all the inventories appear to be underestimating the magnitude of NO_x emissions. We have two hypotheses for this magnitude disagreement. This could be indicative of an error in the inventory caused by a large fraction of diesel vehicles in these countries, which are known to have been underestimated in the past (Anenberg *et al* 2017). Another hypothesis is that this could be indicative of daily lifestyle differences which would present itself in the mid-day to 24 h average conversion. For example, if the activities leading to NO_x emissions in



these countries are concentrated in the late morning or early afternoon, and less in the morning or evening due to a heavier reliance on public transit, then the mid-day to 24 h average multiplicative conversion factor should be lower. An additional hypothesis for Europe is that a longer NO_2 lifetime due to Europe's extratropical latitudes is not being fully captured in our method.

In China ($n = 6$), we observe a broad peak in NO_x emissions in the 2009–2012 timeframe, and subsequent reduction since 2012. Between 2012 and 2018, we calculate that urban NO_x emissions decreased 35%, which was similar in magnitude to the urban NO_x reduction between 2006 and 2012 in the United States and Canada (37%). When comparing to the satellite-based estimates, all bottom-up inventories appear to underestimate the rapid decrease in

Chinese NO_x emissions. The CEDS inventory, which uses the regionally-compiled MEIC inventory (Zheng *et al* 2018) with different spatial downscaling proxies, does capture the urban decreases, but not the extent—between 2012 and 2015, the gridded inventory reports a 7% decrease for the cities considered while the satellite data show a 22% decrease over the same 3 year period. On a national scale, reported Chinese NO_x emissions decreased by 17% in the inventory between 2012 and 2015, but this larger decrease was driven by power plants located in rural locations. These findings are consistent with Zheng *et al* (2018) who also report that OMI NO_2 downward trends are larger than the regional bottom-up inventory. They documented that downward trends in surface NO_2 concentrations between 2012 and 2017 are smaller than the downward trends in the emissions



inventory and satellite data; the ultimate reason for the disagreement is still unknown. However, the difference in this study is that we now account for the NO₂ chemical lifetime, which has been documented to change over time and is responsible for some fraction of urban NO₂ changes (Laughner and Cohen 2019).

In the Middle East ($n = 11$), all bottom-up inventories suggest a consistent increase in urban NO_x emissions between 2006 and 2018, but the top-down OMI NO_x estimates do not support this. Instead, the satellite measurements indicate that NO_x emissions peaked in 2009, with a slow decrease in the following years. While urban NO_x emissions still appear to be larger in 2018 than in 2006, the top-down estimate suggests only 10% larger as compared to 40%–60% larger as reported by the inventories. This discrepancy appears to be mostly driven by four cities (Dubai, Riyadh, Jeddah, and Karachi), which have shown relatively flat NO_x emission changes between 2005 and 2018. In Latin America ($n = 11$) and Africa ($n = 6$), the narrative is similar to the Middle East in that projected upwards NO_x emission trends in the later part of the time record (2012–2018) were in fact steady or downward trends. Scant country-level data exists on emissions or their trends for these regions to inform or validate the global inventories.

Top-down urban NO_x emissions are most uncertain in India ($n = 8$). There are many reasons for this. First, the satellite measurements in India, especially Delhi, are most affected by aerosol interference as

compared to other urban areas around the globe (Vohra *et al* 2021). Because of this bias, top-down urban NO_x emissions are likely biased low in this region. Satellite measurements in India are also biased by the wet monsoon (limited measurements) and dry monsoon (long-range transport from biomass burning may influence the urban calculation). Further, Indian bottom-up inventories sometimes show unrealistic changes, such as the 31% drop in the EDGAR-reported Delhi NO_x emissions between 2011 and 2012. Sharp changes in the inventory at the urban scale are likely due to the downscaling/disaggregation of national emissions because national trends do not have similar sharp changes (figure S3). With that said, urban area NO₂ trends are noticeably different when compared to the relatively rural, but highly industrial areas of east central India (Chhattisgarh and Jharkhand). In the largest Indian cities (e.g. Delhi, Mumbai, and Kolkata), NO₂ trends are relatively flat between 2005 and 2019, while there have been large increases in east central India (figure S5). This may suggest an issue in the spatial disaggregation of emissions as opposed to an error in the national inventory.

When summing all urban areas in our study, ($n = 80$), we find that satellite-based measurements show a larger decrease in global urban NO_x emissions than currently reported in the inventories or projections (figure 4). Between 2009 and 2018, the satellite measurements indicate that urban NO_x emissions dropped by 3%–4% yr⁻¹, while the inventories and

projections suggest drops generally less than $2\% \text{ yr}^{-1}$. The OMI observed NO_x reductions in the 2015–2018 timeframe are most similar to the CEDS inventory ($2.2\% \text{ yr}^{-1}$) and the SSP 1–1.9 projection ($2.0\% \text{ yr}^{-1}$) as seen in figure 4. The CEDS inventory captures the recent global decreases best, presumably because it relies more heavily on country-inventory data. ECLIPSE (a projection between 2015 and 2020) and MACCity (a projection throughout the entire timeframe) both show a steady decrease over time ($\sim 1\% \text{ yr}^{-1}$), but fail to capture the dramatic drops starting 2012. The EDGAR inventory likewise does not capture the drop starting in 2012. We attribute this to an underestimation of Chinese decreases as well as slower increases in developing nations such as Latin America and Africa (Hickman *et al* 2021) in the 2012–2018 timeframe.

4. Conclusions

In this study, we calculate anthropogenic urban NO_x emissions and their trends in 80 global megacities during 2005–2019. Generally, top-down and bottom-up urban NO_x emission trends show good agreement in North America, Europe, Korea/Japan, and Australasia. In China, bottom-up inventories fail to capture the timing of urban emission reductions, which appear to have occurred faster in the 2012–2015 timeframe than currently reported. In developing nations (Latin America, Africa, India) it appears that large projected increases in NO_x emissions have not materialized to date. As a result, satellite-based measurements, when aggregated globally, show a larger decrease in urban NO_x emissions than currently reported in the inventories in the 2009–2018 timeframe.

It should be noted that global inventories have to make assumptions about the spatial distribution of sources, such as power plants and vehicles. For example, power plants near urban areas may be more likely to be subject to greater emission controls than those located elsewhere in a country. In addition, passenger and freight vehicles likely have different spatial and temporal distributions. These types of distinctions are less likely to be captured in global gridded datasets, compared to region-specific inventories such as the U.S. National Emissions Inventory. Therefore, a portion of the disagreement may not be due to errors in the national-level inventory, but instead a misallocation of the spatial (and implied temporal) distribution (e.g. Huneus *et al* 2020). Therefore, the NO_x emission trends reported here are specific to the cities studied and are not necessarily reflective of national trends.

The distinct advantage of our methodology is the ability to isolate urban emissions at the global scale, while accounting for lifetime differences driven by meteorology and chemical nonlinearities. Further our method directly accounts for meteorological

(Goldberg *et al* 2020) and chemical lifetime (Laughner and Cohen 2019) differences between regions which are important and can be difficult to disentangle. For example a city in an Equatorial region (e.g. Singapore) will have smaller NO_2 concentrations due to the smaller solar zenith angle and faster photolysis than an extratropical city (e.g. Paris) with equivalent NO_x emissions. Similarly, NO_2 columns can be up to three times smaller on days with winds $> 8 \text{ m s}^{-1}$ as compared to days with winds $< 2 \text{ m s}^{-1}$ given equivalent NO_x emissions (Goldberg *et al* 2020).

However, it should be noted that there is a cross-dependence of fitted effective NO_2 lifetime and satellite-derived NO_x emissions. The derived NO_x emissions reported herein will increase with a shorter effective NO_2 lifetime and decrease with a longer effective NO_2 lifetime, under a scenario of constant NO_2 . The parameters that are used to calculate the NO_2 lifetime are the wind speed and exponential decay length scale, which means that this method is particularly sensitive to wind speed, wind direction, and the sources downwind of an urban area; the latter two variables affect the fitted exponential decay length scale. A consistent low bias in wind speed, for example, would decrease the effective NO_2 lifetime, and increase the derived NO_x emissions. A consistent source downwind of an urban area, such as a smaller city, would increase the effective NO_2 lifetime, and decrease the derived NO_x emissions. Effective NO_2 lifetimes for all cities are provided in table S4.

Future work to reduce the methodological uncertainties should focus on comprehensively testing this method using a global chemical transport model at high spatial resolution. While this has been done previously using a regional model for Atlanta (De Foy *et al* 2014), differences in local conditions can be substantial sources of error and are hard to account for. For example, the air mass factor and local meteorology can vary substantially between cities, and while some effort was made to account for these differences, our assumptions were broad and sometimes used coarse spatial resolution datasets. Better quantifying errors in the winds/plume speed and vertical distribution of NO_2 through *in situ* observations or even satellite data itself (Liu *et al* 2021) at various times of the days will also be crucial to reducing the uncertainty. Long-term records from remote sensing instruments with higher spatial resolution and higher signal-to-noise ratios, such as the Tropospheric Monitoring Instrument (Veefkind *et al* 2012), Tropospheric Emissions: Monitoring Pollution (Zoogman *et al* 2017), Geostationary Environment Monitoring Spectrometer (Choi 2018), will further reduce the uncertainties in our top-down emissions method and provide estimates at higher temporal (daily/monthly) resolution (Griffin *et al* 2019, Lorente *et al* 2019, Goldberg *et al* 2019b, 2021). Future applications of this technique may be valuable for urban policymakers who want to better quantify changes in their

air quality footprint over decadal timeframes, and track progress towards policy goals. Satellite datasets, as a stand-alone product, should not be used to determine compliance, but instead could be used as one of many metrics to assess progress.

Data availability statement

The data that support the findings of this study are openly available at the following URL/DOI: <https://doi.org/10.6084/m9.figshare.14807565>. Data will be available from 18 October 2021.

Acknowledgments

This publication was developed using funding from the NASA Atmospheric Composition Modeling and Analysis Program (ACMAP) (80NSSC19K0946), NASA Health and Air Quality (HAQ) program (80NSSC19K0193), and NASA Health and Air Quality Applied Sciences Team (HAQAST) (80NSSC21K0511). This publication was also partially funded by the Department of Energy, Office of Fossil Energy and Carbon Management. OMI NO₂ data can be freely downloaded from the NASA website (doi: 10.5067/Aura/OMI/DATA2017). ERA5 re-analysis hourly data on single levels can be downloaded from Copernicus Climate Change Service (doi: 10.24381/cds.adbb2d47).

ORCID iDs

Daniel L Goldberg  <https://orcid.org/0000-0003-0784-3986>
 Susan C Anenberg  <https://orcid.org/0000-0002-9668-603X>
 Zifeng Lu  <https://orcid.org/0000-0001-7331-5861>
 David G Streets  <https://orcid.org/0000-0002-0223-1350>
 Erin E McDuffie  <https://orcid.org/0000-0002-6845-6077>
 Steven J Smith  <https://orcid.org/0000-0003-3248-5607>

References

- Abad G G *et al* 2019 Five decades observing Earth's atmospheric trace gases using ultraviolet and visible backscatter solar radiation from space *J. Quant. Spectrosc. Radiat. Transfer* **238** 106478
- Achakulwisut P, Brauer M, Hystad P and Anenberg S C 2019 Global, national, and urban burdens of paediatric asthma incidence attributable to ambient NO₂ pollution: estimates from global datasets *Lancet Planet Heal.* **3** e166–78
- Anenberg S C *et al* 2017 Impacts and mitigation of excess diesel-related NO_x emissions in 11 major vehicle markets *Nature* **545** 467–71
- Barkley P M, González Abad G, Kurosu P T, Spurr R, Torbatian S and Lerot C 2017 OMI air-quality monitoring over the Middle East *Atmos. Chem. Phys.* **17** 4687–709
- Beirle S, Boersma K F, Platt U, Lawrence M G and Wagner T 2011 Megacity emissions and lifetimes of nitrogen oxides probed from space *Science* **333**
- Burrows J P *et al* 1999 The global ozone monitoring experiment (GOME): mission concept and first scientific results *J. Atmos. Sci.* **56** 151–75
- Canty T P, Hembeck L, Vinciguerra T P, Anderson D C, Goldberg D L, Carpenter S F, Allen D J, Loughner C P, Salawitch R J and Dickerson R R 2015 Ozone and NO_x chemistry in the eastern US: evaluation of CMAQ/CB05 with satellite (OMI) data *Atmos. Chem. Phys.* **15** 10965–82
- Castellanos P and Boersma K F 2012 Reductions in nitrogen oxides over Europe driven by environmental policy and economic recession *Sci. Rep.* **2** 1–7
- Choi W J 2018 Introducing the geostationary environment monitoring spectrometer *J. Appl. Remote Sens.* **12** 1
- Cooper M J, Martin R V, Padmanabhan A and Henze D K 2017 Comparing mass balance and adjoint methods for inverse modeling of nitrogen dioxide columns for global nitrogen oxide emissions *J. Geophys. Res.* **122** 4718–34
- Crippa M, Solazzo E, Huang G, Guizzardi D, Koffi E, Muntean M, Schiebele C, Friedrich R and Janssens-Maenhout G 2020 High resolution temporal profiles in the emissions database for global atmospheric research *Sci. Data* **7** 121
- De Foy B, Lu Z and Streets D G 2016 Satellite NO₂ retrievals suggest China has exceeded its NO_x reduction goals from the twelfth Five-Year Plan *Sci. Rep.* **6** 1–9
- De Foy B, Lu Z, Streets D G, Lamsal L N and Duncan B N 2015 Estimates of power plant NO_x emissions and lifetimes from OMI NO₂ satellite retrievals *Atmos. Environ.* **116** 1–11
- De Foy B, Wilkins J L, Lu Z, Streets D G and Duncan B N 2014 Model evaluation of methods for estimating surface emissions and chemical lifetimes from satellite data *Atmos. Environ.* **98** 66–77
- Denier Van Der Gon H, Hendriks C, Kuenen J, Segers A and Visschedijk A 2011 Description of current temporal emission patterns and sensitivity of predicted AQ for temporal emission patterns EU FP7 MACC deliverable report D_D-EMIS_1.3 (available at: https://atmosphere.copernicus.eu/sites/default/files/2019-07/MACC_TNO_del_1_3_v2.pdf)
- Dobber M, Kleipool Q, Dirksen R, Levelt P F, Jaross G, Taylor S, Kelly T, Flynn L, Leppelmeier G and Rozemeijer N 2008 Validation of ozone monitoring instrument level 1b data products *J. Geophys. Res.* **113** D15S06
- Duncan B N, Lamsal L N, Thompson A M, Yoshida Y, Lu Z, Streets D G, Hurwitz M M and Pickering K E 2016 A space-based, high-resolution view of notable changes in urban NO_x pollution around the world (2005–2014) *J. Geophys. Res. Atmos.* **121** 976–96
- Duncan B N, Yoshida Y, De Foy B, Lamsal L N, Streets D G, Lu Z, Pickering K E and Krotkov N A 2013 The observed response of ozone monitoring instrument (OMI) NO₂ columns to NO_x emission controls on power plants in the United States: 2005–2011 *Atmos. Environ.* **81** 102–11
- Elguindi N *et al* 2020 Intercomparison of magnitudes and trends in anthropogenic surface emissions from bottom-up inventories, top-down estimates, and emission scenarios *Earth's Future* **8** e2020EF001520
- Gauderman W J, Avol E, Lurmann F, Kuenzli N, Gilliland F, Peters J and McConnell R 2005 Childhood asthma and exposure to traffic and nitrogen dioxide *Epidemiology* **16** 737–43
- Geddes J A, Martin R V, Boys B L and Van Donkelaar A 2016 Long-term trends worldwide in ambient NO₂ concentrations inferred from satellite observations *Environ. Health Perspect.* **124** 281–9
- Georgoulas A K, Van Der A R J, Stammes P, Boersma K F and Eskes H J 2019 Trends and trend reversal detection in 2 decades of tropospheric NO₂ satellite observations *Atmos. Chem. Phys.* **19** 6269–94

- Goldberg D L *et al* 2019c A top-down assessment using OMI NO₂ suggests an underestimate in the NO_x emissions inventory in Seoul, South Korea, during KORUS-AQ *Atmos. Chem. Phys.* **19** 1801–18
- Goldberg D L, Anenberg S C, Griffin D, McLinden C A, Lu Z and Streets D G 2020 Disentangling the impact of the COVID-19 lockdowns on urban NO₂ from natural variability *Geophys. Res. Lett.* **47** e2020GL089269
- Goldberg D L, Anenberg S C, Kerr G H, Moheggh A, Lu Z and Streets D G 2021 TROPOMI NO₂ in the United States: a detailed look at the annual averages, weekly cycles, effects of temperature, and correlation with surface NO₂ concentrations *Earth's Futur.* **9** e2020EF001665 (available at: <https://onlinelibrary.wiley.com/doi/10.1029/2020EF001665>)
- Goldberg D L, Lu Z, Oda T, Lamsal L N, Liu F, Griffin D, McLinden C A, Krotkov N A, Duncan B N and Streets D G 2019a Exploiting OMI NO₂ satellite observations to infer fossil-fuel CO₂ emissions from U.S. megacities *Sci. Total Environ.* **695** 133805
- Goldberg D L, Lu Z, Streets D G, De Foy B, Griffin D, McLinden C A, Lamsal L N, Krotkov N A and Eskes H 2019b Enhanced capabilities of TROPOMI NO₂: estimating NO_x from North American cities and power plants *Environ. Sci. Technol.* **9** 12594–601 (available at: <https://pubs.acs.org/doi/10.1021/acs.est.9b04488>)
- Griffin D *et al* 2019 High-resolution mapping of nitrogen dioxide with TROPOMI: first results and validation over the Canadian oil sands *Geophys. Res. Lett.* **46** 1049–60
- Harkey M, Holloway T, Oberman J and Scotty E 2015 An evaluation of CMAQ NO₂ using observed chemistry-meteorology correlations *J. Geophys. Res. Atmos.* **120** 11775–97
- He M Z, Kinney P L, Li T, Chen C, Sun Q, Ban J, Wang J, Liu S, Goldsmith J and Kioumourtoglou M A 2020 Short- and intermediate-term exposure to NO₂ and mortality: a multi-county analysis in China *Environ. Pollut.* **261** 114165
- Hersbach H *et al* 2020 The ERA5 global reanalysis *Q. J. R. Meteorol. Soc.* **146** 1999–2049
- Hickman J E, Andela N, Tsigaridis K, Galy-Lacaux C, Ossouhou M and Bauer S E 2021 Reductions in NO₂ burden over north equatorial Africa from decline in biomass burning in spite of growing fossil fuel use, 2005–2017 *Proc. Natl Acad. Sci.* **118** e2002579118
- Huneus N *et al* 2020 Evaluation of anthropogenic air pollutant emission inventories for South America at national and city scale *Atmos. Environ.* **235** 117606
- Itahashi S, Yumimoto K, Kurokawa J, Morino Y, Nagashima T, Miyazaki K, Maki T and Ohara T 2019 Inverse estimation of NO_x emissions over China and India 2005–2016: contrasting recent trends and future perspectives *Environ. Res. Lett.* **14** 124020
- Jacob D J 1999 *Introduction to Atmospheric Chemistry* (available at: <http://acmg.seas.harvard.edu/people/faculty/djj/book/>)
- Jacob D J 2000 Heterogeneous chemistry and tropospheric ozone *Atmos. Environ.* **34** 2131–59
- Khreis H, Kelly C, Tate J, Parslow R, Lucas K and Nieuwenhuijsen M 2017 Exposure to traffic-related air pollution and risk of development of childhood asthma: a systematic review and meta-analysis *Environ. Int.* **100** 1–31
- Kim S-W, Heckel A, Frost G J, Richter A, Gleason J, Burrows J P, McKeen S A, Hsieh E-Y-Y, Granier C and Trainer M K 2009 NO₂ columns in the western United States observed from space and simulated by a regional chemistry model and their implications for NO_x emissions *J. Geophys. Res. Atmos.* **114** D11301
- Kimbrough S, Chris Owen R, Snyder M and Richmond-Bryant J 2017 NO to NO₂ conversion rate analysis and implications for dispersion model chemistry methods using Las Vegas, Nevada near-road field measurements *Atmos. Environ.* **165** 23–34
- Klimont Z, Kupiainen K, Heyes C, Purohit P, Cofala J, Rafaj P, Borken-Kleefeld J and Schöpp W 2017 Global anthropogenic emissions of particulate matter including black carbon *Atmos. Chem. Phys.* **17** 8681–723
- Krotkov N A *et al* 2016 Aura OMI observations of regional SO₂ and NO₂ pollution changes from 2005 to 2015 *Atmos. Chem. Phys.* **16** 4605–29
- Krotkov N A, Lamsal L N, Celarier E A, Swartz W H, Marchenko S V, Bucsela E J, Chan K L, Wenig M O and Zara M 2017 The version 3 OMI NO₂ standard product *Atmos. Meas. Tech.* **10** 3133–49
- Lamarque J-F *et al* 2010 Historical (1850–2000) gridded anthropogenic and biomass burning emissions of reactive gases and aerosols: methodology and application *Atmos. Chem. Phys.* **10** 7017–39
- Lamsal L N *et al* 2021 Ozone Monitoring Instrument (OMI) Aura nitrogen dioxide standard product version 4.0 with improved surface and cloud treatments *Atmos. Meas. Tech.* **14** 455–79
- Lamsal L N, Martin R V, Padmanabhan A, Van Donkelaar A, Zhang Q, Sioris C E, Chance K V, Kurosu T P and Newchurch M J 2011 Application of satellite observations for timely updates to global anthropogenic NO_x emission inventories *Geophys. Res. Lett.* **38** 1–5
- Laughner J L and Cohen R C 2019 Direct observation of changing NO_x lifetime in North American cities *Science* **366** 723–7
- Leue C, Wenig M, Wagner T, Klimm O, Platt U and Jähne B 2001 Quantitative analysis of NO_x emissions from global ozone monitoring experiment satellite image sequences *J. Geophys. Res. Atmos.* **106** 5493–505
- Levelt P F *et al* 2018 The ozone monitoring instrument: overview of 14 years in space *Atmos. Chem. Phys.* **18** 5699–745
- Levelt P F, Van Den Oord G H J, Dobber M R, Dirksen R J, Mäkelä A, Visser H, De Vries J, Stammes P, Lundell J O V and Saari H 2006 The ozone monitoring instrument *IEEE Trans. Geosci. Remote Sens.* **44** 1093–101
- Li M, Klimont Z, Zhang Q, Martin R V, Zheng B, Heyes C, Cofala J, Zhang Y and He K 2018 Comparison and evaluation of anthropogenic emissions of SO₂ and NO_x over China *Atmos. Chem. Phys.* **18** 3433–56
- Liu F *et al* 2018 A new global anthropogenic SO₂ emission inventory for the last decade: a mosaic of satellite-derived and bottom-up emissions *Atmos. Chem. Phys.* **18** 16571–86
- Liu F, Duncan B N, Krotkov N A, Lamsal L N, Beirle S, Griffin D, McLinden C A, Goldberg D L and Lu Z 2020 A methodology to constrain carbon dioxide emissions from coal-fired power plants using satellite observations of co-emitted nitrogen dioxide *Atmos. Chem. Phys.* **20** 99–116
- Liu X, Mizzi A P, Anderson J L, Fung I and Cohen R C 2021 The potential for geostationary remote sensing of NO₂ to improve weather prediction *Atmos. Chem. Phys.* **21** 9573–83
- Lorente A, Boersma K F, Eskes H J, Veefkind J P, Van Geffen J H G M, De Zeeuw M B, Denier Van Der Gon H A C, Beirle S and Krol M C 2019 Quantification of nitrogen oxides emissions from build-up of pollution over Paris with TROPOMI *Sci. Rep.* **9** 20033
- Lu Z and Streets D G 2012 Increase in NO_x emissions from Indian thermal power plants during 1996–2010: unit-based inventories and multisatellite observations *Environ. Sci. Technol.* **46** 7463–70
- Lu Z, Streets D G, De Foy B, Lamsal L N, Duncan B N and Xing J 2015 Emissions of nitrogen oxides from US urban areas: estimation from ozone monitoring instrument retrievals for 2005–2014 *Atmos. Chem. Phys.* **15** 10367–83
- Macdonald E, Otero N and Butler T 2021 A comparison of long-term trends in observations and emission inventories of NO_x *Atmos. Chem. Phys.* **21** 4007–23
- Mahajan A S, De Smedt I, Biswas M S, Ghude S, Fadnavis S, Roy C and Van Roozendaal M 2015 Inter-annual variations in satellite observations of nitrogen dioxide and formaldehyde over India *Atmos. Environ.* **116** 194–201

- Marchenko S V, Krotkov N A, Lamsal L N, Celarier E A, Swartz W H and Bucsela E J 2015 Revising the slant column density retrieval of nitrogen dioxide observed by the ozone monitoring instrument *J. Geophys. Res. Atmos.* **120** 5670–92
- Martin R V 2003 Global inventory of nitrogen oxide emissions constrained by space-based observations of NO₂ columns *J. Geophys. Res.* **108** 4537
- McDuffie E E, Smith S J, O'Rourke P, Tibrewal K, Venkataraman C, Marais E A, Zheng B, Crippa M, Brauer M and Martin R V 2020 A global anthropogenic emission inventory of atmospheric pollutants from sector- and fuel-specific sources (1970–2017): an application of the community emissions data system (CEDS) *Earth Syst. Sci. Data* **12** 3413–42
- McLinden C A, Fioletov V E, Shephard M W, Krotkov N, Li C, Martin R V, Moran M D and Joiner J 2016 Space-based detection of missing sulfur dioxide sources of global air pollution *Nat. Geosci.* **9** 496–500
- Qu Z, Henze D K, Cooper O R and Neu J L 2020 Impacts of global NO_x inversions on NO₂ and ozone simulations *Atmos. Chem. Phys.* **20** 13109–30
- Reuter M, Buchwitz M, Hilboll A, Richter A, Schneising O, Hilker M, Heymann J, Bovensmann H and Burrows J P 2014 Decreasing emissions of NO_x relative to CO₂ in East Asia inferred from satellite observations *Nat. Geosci.* **7** 792–5
- Riahi K et al 2017 The Shared Socioeconomic Pathways and their energy, land use, and greenhouse gas emissions implications: an overview *Glob. Environ. Change.* **42** 153–68
- Richter A and Burrows J P 2002 Tropospheric NO₂ From GOME Measurements **29** (available at: www.elsevier.com/locate/lastr)
- Richter A, Burrows J P, Nüß H, Granier C and Niemeier U 2005 Increase in tropospheric nitrogen dioxide over China observed from space *Nature* **437** 129–32
- Ritchie H and Roser M 2018 Urbanization *Our World Data*
- Russell A R, Valin L C, Bucsela E J, Wenig M O and Cohen R C 2010 Space-based constraints on spatial and temporal patterns of NO_x emissions in California, 2005–2008 *Environ. Sci. Technol.* **44** 3608–15
- Samoli E 2006 Short-term effects of nitrogen dioxide on mortality: an analysis within the APHEA project *Eur. Respir. J.* **27** 1129–38
- Shen L et al 2019 The 2005–2016 trends of formaldehyde columns over china observed by satellites: increasing anthropogenic emissions of volatile organic compounds and decreasing agricultural fire emissions *Geophys. Res. Lett.* **46** 2019GL082172 (available at: <https://online.library.wiley.com/doi/abs/10.1029/2019GL082172>)
- Silvern R F et al 2019 Using satellite observations of tropospheric NO₂ columns to infer long-term trends in US NO_x emissions: the importance of accounting for the free tropospheric NO₂ background *Atmos. Chem. Phys.* **19** 8863–78
- Stavrakou T, Müller J-F, Boersma K F, De Smedt I and Van Der A R J 2008 Assessing the distribution and growth rates of NO_x emission sources by inverting a 10-year record of NO₂ satellite columns *Geophys. Res. Lett.* **35** L10801
- Valin L C, Russell A R and Cohen R C 2013 Variations of OH radical in an urban plume inferred from NO₂ column measurements *Geophys. Res. Lett.* **40** 1856–60
- Valin L C, Russell A R, Hudman R C and Cohen R C 2011 Effects of model resolution on the interpretation of satellite NO₂ observations *Atmos. Chem. Phys.* **11** 11647–55
- Veefkind J P et al 2012 TROPOMI on the ESA Sentinel-5 Precursor: a GMES mission for global observations of the atmospheric composition for climate, air quality and ozone layer applications *Remote Sens. Environ.* **120** 70–83
- Verstraeten W W, Boersma K F, Douros J, Williams J E, Eskes H, Liu F, Beirle S and Delcloo A 2018 Top-down NO_x emissions of european cities based on the downwind plume of modelled and space-borne tropospheric NO₂ columns *Sensors* **18** 2893
- Visser A J, Folkert Boersma K, Ganzeveld L N and Krol M C 2019 European NO_x emissions in WRF-Chem derived from OMI: impacts on summertime surface ozone *Atmos. Chem. Phys.* **19** 11821–41
- Vohra K et al 2021 Long-term trends in air quality in major cities in the UK and India: a view from space *Atmos. Chem. Phys.* **21** 6275–96
- Wang C, Wang T and Wang P 2019 The spatial-temporal variation of tropospheric NO₂ over China during 2005–2018 *Atmosphere (Basel)* **10** 444
- Zara M, Boersma K F, Eskes H, Denier Van Der Gon H, Vilà-guerau De Arellano J, Krol M, Van Der Swaluw E, Schuch W and Velders G J M 2021 Reductions in nitrogen oxides over the Netherlands between 2005 and 2018 observed from space and on the ground: decreasing emissions and increasing O₃ indicate changing NO_x chemistry *Atmos. Environ.* **X** 9 100104 (available at: <https://linkinghub.elsevier.com/retrieve/pii/S2590162121000046>)
- Zhang R, Wang Y, Smeltzer C, Qu H, Koshak W and Folkert Boersma K 2018 Comparing OMI-based and EPA AQS *in situ* NO₂ trends: towards understanding surface NO_x emission changes *Atmos. Meas. Tech.* **11** 3955–67
- Zheng B et al 2018 Trends in China's anthropogenic emissions since 2010 as the consequence of clean air actions *Atmos. Chem. Phys.* **18** 14095–111
- Zoogman P et al 2017 Tropospheric emissions: monitoring of pollution (TEMPO) *J. Quant. Spectrosc. Radiat. Transfer* **186** 17–39